(ORNL/Sub/93-SP173/04)

STUDY OF FATIGUE AND FRACTURE BEHAVIOR OF CR-BASED ALLOYS AND INTERMETALLIC MATERIALS:

Effects of Processing on the Microstructure and Mechanical Behavior of Binary Cr-Ta Alloys

January 18, 2001

Report Prepared by

Y. H. He, Y. Lu, D. F. Wang, and P. K. Liaw

The University of Tennessee,
Department of Materials Science and Engineering
Knoxville, TN 37996-2200

and

C. T. Liu, L. Heatherley, and E. P. George

Oak Ridge National Laboratory
Oak Ridge, TN 37831-6115

under

Subcontract No.: 11X-SP173V, UT-2(A)

for

OAK RIDGE NATIONAL LABORATORY
Oak Ridge, Tennessee 37831
Managed by
UT-BATTELLE, LLC
for the
U. S. DEPARTMENT OF ENERGY
under contract DE-AC05-00OR22725

(ORNL/Sub/93-SP173/04)

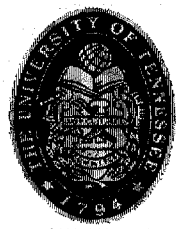

STUDY OF FATIGUE AND FRACTURE BEHAVIOR OF CR-BASED ALLOYS AND INTERMETALLIC MATERIALS:

Effects of Processing on the Microstructure and Mechanical Behavior of Binary Cr-Ta Alloys

January 18, 2001

Research sponsored by the U. S. Department of Energy,
Office of Fossil Energy
Advanced Research Materials Program

Report Prepared by

Y. H. He, Y. Lu, D. F. Wang, and P. K. Liaw

The University of Tennessee,
Department of Materials Science and Engineering
Knoxville, TN 37996-2200

and

C. T. Liu, L. Heatherley, and E. P. George

Oak Ridge National Laboratory
Oak Ridge, TN 37831-6115

under

Subcontract No.: 11X-SP173V, UT-2(A)

for

OAK RIDGE NATIONAL LABORATORY
Oak Ridge, Tennessee 37831
Managed by
UT-BATTELLE, LLC
for the
U. S. DEPARTMENT OF ENERGY
under contract DE-AC05-00OR22725

EFFECTS OF PROCESSING ON THE MICROSTRUCTURE AND MECHANICAL BEHAVIOR OF BINARY Cr-Ta ALLOYS *

Y. H. He, Y. Lu, D. F. Wang, and P. K. Liaw
Materials Science and Engineering Department
The University of Tennessee
Knoxville, TN 37996-2200
and
C. T. Liu, L. Heatherly, and E. P. George
Metals and Ceramics Division
Oak Ridge National Laboratory
Oak Ridge, TN 37831-6115

Abstract

The microhardness, and tensile and fracture-toughness properties of drop-cast and directionally-solidified Cr-9.25 at.% (atomic percent) Ta alloys have been investigated. Directional solidification was found to soften the alloy, which could be related to the development of equilibrium and aligned microstructures. It was observed that the tensile properties of the Cr-Ta alloys at room and elevated temperatures could be improved by obtaining aligned microstructures. The directionally-solidified alloy also showed increased fracture toughness at room temperature. This trend is mainly associated with crack deflection and the formation of shear ribs in the samples with aligned microstructures. The sample with better-aligned lamellar exhibits greater fracture toughness.

* Research sponsored by the U.S. Department of Energy, Fossil Energy Advanced Research Materials Program, DOE/FE AA 15 10 10 0, Work Breakdown Structure Element UT-2(A)

Introduction

The Cr_2X (X = Ti, Hf, Zr, Nb, Ta, etc.) Laves-phase alloys are candidate materials for applications at temperatures greater than 1,200°C, because these alloys have good oxidation resistance and strength at elevated temperatures.[1-7] However, these alloys are very brittle at room (24°C) and moderately high temperatures (400 to 800°C), which prohibits their commercial applications as structural materials. One of the potential solutions to overcome the brittleness of Laves-phase alloys is to fabricate in-situ composites containing reinforcing Laves phases in a relatively ductile matrix.[8-15] The presence of a Cr-Cr_2Ta eutectic reaction provides a good opportunity for the formation of a Cr solid solution alloy reinforced with the Cr_2Ta Laves phase.[16] The Cr-Cr_2Ta alloy has a melting point greater than 1,700°C, and the Laves phase has an ordered crystal structure so that it shows excellent mechanical properties at elevated temperatures. In addition, the Cr matrix phase exhibits some ductility, which is greater than that of the Cr_2Ta Laves phase at room temperature,[3, 17] and good oxidation resistance at elevated temperatures. The mechanical properties of the Cr matrix can be improved by thermomechanical treatment and alloying-element additions.[17-19] Thus, the Cr solid solution matrix composites reinforced by Laves phases makes the material attractive. However, only limited work has been performed on the Cr solid-solution matrix based in-situ composites reinforced by the Cr_2Ta Laves phase.[7, 13, 15] In this work, the improvement of mechanical properties of the alloy was achieved by the formation of aligned microstructures using a high-temperature optical floating zone furnace.

Experimental Materials and Method

High-purity Cr and Ta chips were used as charge materials in order to avoid deleterious effects of impurities on the microstructure and mechanical properties of the alloys. The nominal composition of the alloy studied is Cr-9.25 at.% Ta. Button-shaped samples of the alloy were obtained by arc-melting in argon. Every sample was inverted and re-melted more than ten times in order to improve the homogeneity of the microstructure and chemical composition of the alloy. Then cylindrical ingots with a length of 60 mm and a diameter of 9 mm were obtained by drop-casting. The loss of weight is less than 0.5 wt.% (weight percent) during the entire fabrication process of the alloy, which is mainly related to the evaporation of Cr. The samples with aligned microstructures were made by directional solidification using a high-temperature optical floating zone furnace. The directionally-solidified samples were grown in flowing argon. The effect of growth conditions, including the growing speed and rotation rate, has been determined previously.[20] Selected samples were heat treated in vacuum before mechanical tests. The heat-treatment condition was 1,200°C/1 day (d) + 1,100°C/1 day (d) + 900°C/2 days (ds).

The microstructures and fracture surfaces of the alloy were examined using optical microscopy (OM) and scanning-electron microscopy (SEM: Cambridge Instrument S360). The samples for microstructural examination were electrolytically etched in a solution of the 100-grams oxalic acid and 1,000 ml-pure water for 30 seconds, with a voltage of 10 V, and current of 4 A. The microhardness was measured on polished samples using a Micronet 2001 Microhardness Tester with a load of 1,000 grams.

Tensile tests were conducted at room temperature and elevated temperatures of 800°C and 1,000°C in air using an Instron testing machine equipped with an induction heater. Samples with gage dimensions of 1.5 × 3.0 × 25.3 mm were fabricated with an electric-discharge machine (EDM), and polished using grinding papers with grits from 180 down to 600. For the directionally-solidified Cr-Ta alloy samples, the tensile loading direction

was parallel to the growth direction of the samples. The loading rate was 2 mm/min, which corresponds to a strain rate of 1.3×10^{-3}/s.

Subsized chevron-notched three-point bend samples with dimensions of $2.5 \times 3.5 \times 25$ mm were used to determine the fracture toughness of the Cr-Ta alloys. The bend tests were performed on an Instron testing machine at room temperature. The cross-head speed was 10 μm/s. The chevron-notch has a triangular shape with a width of 2 mm and height of 1.8 mm. Therefore, the chevron-notch tip bears the maximum tensile stress so that the crack initiates at the tip. The growth direction of the directionally-solidified Cr-Ta alloy was perpendicular to the loading direction during the fracture-toughness tests. The fracture toughness was calculated using the following equation:

$$Kq = (G \times E')^{1/2}$$

where, $G = W/A$, W is the absorbed energy, (i.e., the area of load versus displacement);
A is the area of the triangle through which the crack propagates;
$E' = E/(1-\nu^2)$ is the plane-strain Young's modulus, and ν is Poisson's ratio.

Following the mechanical tests, microstructural characterizations of the tested samples were utilized to provide a mechanistic understanding of the influence of the processing method and the resulting microstructure on the mechanical performance of the alloy.

Results

Microstructures of Processed Material

Figure 1 shows the microstructures of the drop-cast and the directionally-solidified Cr-9.25 at.% Ta alloy samples. The drop-cast alloy has primary Cr solid-solution grains and eutectic colonies, as shown in Fig. 1(a). After the heat treatment described in the experimental section, no change in microstructure could be observed using OM and SEM. By employing directional solidification, an aligned microstructure was obtained at a growth speed of 100 mm/h, as shown in Fig. 1(b). However, there were some growth defects (non-lamellar regions) of about 8-9 vol.% (volume percent) produced during directional solidification at low growth speeds (≤ 80 mm/h). Figure 2 exhibits the cross-sectional microstructure of the directionally-solidified alloy. It can be seen that the Cr_2Ta Laves phase exhibits two kinds of shapes, lamellar and rod-like.

Mechanical Behavior

Table 1 shows the effect of the processing method on the microhardness of the alloy. The drop-cast alloy exhibited the highest microhardness, with heat treatment resulting in

Table 1. Microhardness of the Cr-9.25 at.% Ta alloy

Processing Method	Sample 1 (Vickers)	Sample 2 (Vickers)	Sample 3 (Vickers)	Sample 4 (Vickers)	Sample 5 (Vickers)	Average (Vickers)
DC[(1)]	536	589	532	536	570	553 ± 25
DC + HT[(2)]	448	428	436	451	452	443 ± 10
DS[(3)]	384	380	394	388	388	387 ± 5
DS + HT	373	382	386	384	390	383 ± 6

[(1)] Drop cast
[(2)] Heat treatment: 1,200°C/1d + 1,100°C/1d + 900°C/2ds
[(3)] Directional solidification: 100 mm/h at 20 rpm

significant softening. The lowest microhardness was obtained in the directionally-solidified alloy, and its hardness decreased only slightly after heat treatment.

Table 2 exhibits the influence of the processing method on the tensile properties of the alloy at room and elevated temperatures. The drop-cast sample fractured without yielding at all test temperatures (up to 1,000°C). However, its fracture strength increased with increasing temperature. The fracture strengths can be improved by heat treatment at all three temperatures investigated. At the highest temperature, 1,000°C, limited plastic deformation was obtained along with a high ultimate strength. Among the different processing techniques listed in Table 2, the directionally-solidified and heat-treated alloy exhibited the best tensile properties at the three temperatures. Yielding was observed at 800°C. At the highest temperature of 1,000°C, the directionally-solidified alloy exhibited a combination of good yield and ultimate strengths and ductility.

Table 2 Tensile properties of the Cr-9.25 at.% Ta alloy

Processing Method	Test Temperatures (°C)	Yield Strength (MPa)	Ultimate Strength (MPa)	Total Elongation (%)
DC	24	-	85	0
	800	-	244	0
	1,000	-	330	0
DC + HT	24	-	131	0
	800	-	313	0
	1,000	335	428	0.9
DS + HT	24	-	352	0
	800	350	448	0.8
	1,000	487	573	1.6

The effect of processing on fracture toughness is shown in Table 3. The drop-cast alloy possessed a low fracture toughness at room temperature, which is the main obstacle to

commercial applications of the Cr-Ta alloys. Heat treatment slightly decreased the fracture toughness. The samples of both the drop-cast, and the drop-cast and heat-treated alloys showed very similar fracture toughness values. The fracture toughness was improved by directional solidification.

Table 3 Fracture toughness of the Cr-9.25 at.% Ta alloys at room temperature

Processing Method	Sample 1 $MPa \cdot m^{1/2}$	Sample 2 $MPa \cdot m^{1/2}$	Sample 3 $MPa \cdot m^{1/2}$	Average $MPa \cdot m^{1/2}$
DC	10.2	10.2	10.2	10.2 ± 0.0
DC + HT	9.2	9.5	9.3	9.3 ± 0.1
DS + HT	> 15.0	13.0	11.4	$> 13.1 \pm 1.5$

Microstructures of Tested Samples

To study the effect of microstructure on the tensile properties, the fracture surfaces were examined by SEM. Figure 3 shows the fracture surfaces of the drop-cast and the directionally-solidified Cr-9.25 at.% Ta alloys tensile-tested at room temperature. The fracture surfaces of the drop-cast alloy were relatively smooth; they were identified as cleavage-type fracture. It can be seen that different grains showed different lamellar spacings on the fracture surface, which is due to the different orientations of grains in the drop-cast alloy. Note that the eutectic Cr_2Ta Laves-phase plates are represented in white color, while the eutectic Cr phase plate in gray color. In addition, some microcracks were observed on the fracture surface, as marked by arrows A and B in Fig. 3(a). These microcracks generally propagated along the weak eutectic colony boundaries. In the directionally-solidified alloy, the lamellar spacing was uniformly distributed on the fracture surface, as shown in Fig. 3(b). There were numerous shear ribs in the directionally-solidified alloy, as marked by arrow C in Fig. 3(b). The shear ribs indicate the possibility that cracking occurs at different elevations, and crack deflection can take place.

To observe the crack-propagation characteristics, the microstructure in a plane parallel to the loading direction of the tensile-tested samples was examined using SEM. In the directionally-solidified alloy tensile-tested at room temperature, there are some microcracks, which propagated in the lamellar colonies with crack branching and deflection, as shown in Figure 4. The deflected crack tends to grow along the Cr_2Ta/Cr interface. Note that deflected crack in Fig. 4 could be observed as shear ribs on the fracture surface [Fig. 3(b)].

Upon increasing the test temperature to 1,000°C, microcracks, which mainly propagated along the weak eutectic colony boundaries, were found in the drop-cast alloy, as shown in Fig. 5(a). There were many microcracks in the brittle Cr_2Ta Laves phase along with the deflected cracks in the directionally-solidified alloy, as observed in Fig. 5(b). The presence of the microcracks in the Cr_2Ta Laves phase and crack deflection in the directionally-solidified alloy help absorb fracture energy, and decrease the stress intensity factors around crack tips, thus, increasing the strength and ductility, relative to the drop-cast material.

Fracture surfaces of the fracture-toughness samples were also examined using SEM. The fracture surface of the drop-cast alloy mainly exhibited cleavage features and was generally flat, as shown in Fig. 6(a). In contrast, there were numerous shear ribs in the directionally-solidified alloy as seen in Figs. 6(b) and (c), which results from crack deflection and produces high toughness values (Table 3). In Figs. 6(b) and (c), it can be seen that the microstructure of the directionally-solidified alloy contains aligned Cr_2Ta Laves-phase lamellae and rods. Note that no de-bonding at the Cr_2Ta/Cr interface was observed.

Figures 7(a) and (b) show the microstructures near the chevron-notch tips of the directionally-solidified samples with fracture toughness values of 13.0 $MPa{\cdot}m^{1/2}$ and > 15.0 $MPa{\cdot}m^{1/2}$, respectively. It can be seen that there were more Cr_2Ta Laves-phase lamellae near the notch tip of the sample with the fracture toughness value of > 15.0 $MPa{\cdot}m^{1/2}$ than in the sample with the fracture toughness value of 13.0 $MPa{\cdot}m^{1/2}$. It was

also found that the fracture surface of the sample with a higher fracture toughness value was rough, and contained many shear ribs near the notch tip. Other parts of the microstructures were basically similar in the two samples.

Discussion

From the above results, it can be seen that the mechanical properties of the Cr-9.25 at.% Ta alloy depend on the processing methods and microstructures. Specifically, the microhardness was affected by the processing techniques and microstructural features. The drop-cast alloy showed the highest microhardness. Heat treatment reduced the microhardness of the alloy. The alloy fabricated by directional solidification possessed the lowest microhardness, which may be related to its equilibrium and aligned microstructures. As a result, the heat treatment following directional solidification decreases the microhardness only slightly.

Directional solidification improved the tensile properties of the alloy at room and elevated temperatures, as shown in Table 2. This trend results from the softening behavior produced by the aligned lamellar eutectic microstructure of the directionally-solidified alloy. When the sample was tensile-loaded along the lamellar orientation, it tended to fail perpendicular to the loading direction. In this case, the main crack intersects more lamellar boundaries so that the crack has difficulty in propagating, and it has to deflect, branch, and create shear ribs, as shown in Figs. 3-5. At the highest test temperature of 1,000°C, the deflection behavior of the main crack, and microcracking in the Cr_2Ta Laves phase, were more pronounced than at 24°C (Figs. 4 and 5). These phenomena help absorb fracture energy and decrease the stress intensity factor around the crack tip, which increases the strength and ductility in the directionally-solidified alloy, relative to the drop-cast material. In addition, the ductility improvement by directional solidification may be associated with the formation of special orientations between the Cr solid-solution phase and the Cr_2Ta Laves phase.

The drop-cast alloy exhibited low fracture toughness due to the inherent brittleness of the alloy and weak eutectic colony boundaries [Fig. 5(a)]. The fracture surface showed typical cleavage features. The heat treatment of 1,200°C/1d + 1,100°C/1d + 900°C/2ds slightly affected the fracture toughness of the drop-cast alloy. It is known that fracture toughness is closely associated with the microstructure of alloys. Compared with the

drop-cast alloy, the fracture toughness could be improved by producing an aligned microstructure. This trend is associated with the fact that the aligned microstructure of the alloy can facilitate crack deflection, resulting in the presence of shear ribs. Besides, the eutectic colony boundary of the alloy is weak in the drop-cast alloy, as shown in Fig. 5(a). Hence, the improvement of the fracture toughness by directional solidification could be attributed to a decrease in the number of weak colony boundaries and the enhancement of crack deflection. The alloy is very brittle at room temperature. Therefore, fracture toughness is sensitive to crack initiation. The higher fracture toughness of a directionally-solidified alloy in Table 3 is mainly related to the presence of the aligned lamellae, in Fig. 7(b). Thus, it can be suggested that higher fracture toughness can be obtained by the production of aligned microstructures in which more or less fully aligned lamellar microstructures are present.

Conclusions

1. The microhardness was affected by the microstructure of the Cr-9.25 at.% Ta alloy, and directional solidification softened the alloy.
2. The tensile properties were significantly improved by obtaining aligned microstructures in the alloy at room and elevated temperatures, which is due to crack deflection and the formation of shear ribs.
3. The aligned microstructure results in improved fracture toughness of the alloy.
4. The alloy exhibited good tensile properties at 1,000°C, especially high tensile strength.

Acknowledgement

The research was supported by the Fossil Energy Advanced Research and Technology Development (AR&TD) Materials Program, U. S. Department of Energy, under subcontract, 11X-SP173V, to the University of Tennessee, and by AR&TD Materials Program, under the contract with DE-AC05-000R22725 with UT-Battelle, LLC. Dr. R. R. Judkins is the contract monitor.

References

1. Livingston J. D., Refractory and Silicide Laves Phases, High-temperature Silicides and Refractory Alloy, Briant C. L., et al., (Eds.), Pittsburgh, MRS, 1994, 395-406.
2. Kumar K. S., Laves-Phase-based Materials: Microstructure, Deformation Modes and Properties, High-Temperature Ordered Intermetallic Alloy, Koch C.C. et al., (Eds.), Pittsburgh, MRS, 1997, 677-688.
3. Kumar K. S. and Liu C. T., Precipitation in a Cr-Cr_2Nb Alloy, Acta Materialia, 1997, 45(9), 3671-3686.
4. Ravichandran K. S., Miracle D. B., and Mendiratta M. G., Microstructure and Mechanical Behavior of Cr-Cr_2Hf in-situ Intermetallic Composites, Metallurgical and Materials Transactions, 1996, 27(A9), 2583-2592.
5. Zhu J. H., Liu C. T., and Liaw P. K., Phase Stability and Mechanical Behavior of Nb Cr_2-based Laves Phase, Intermetallics, 1999, 7(9), 1011-1016.
6. Zhu J. H., Liu C. T., Pike L. M., and Liaw P. K., Thermodynamic Interpretation of the Size Ratio Limits for Laves-Phase Formation, Metallurgical and Materials Transaction, 1999, 30(5A), 1449-1452.
7. Brady M. P., Zhu J. H., Liu C. T., Tortorelli P. F., and Walker L. R., Oxidation Resistance and Mechanical Properties of Laves-Phase Reinforced Cr in-situ Composites, Intermetallics, 2000, 0, 1-8.
8. Aoyama N. and Hanada S., Microstructure and Strength of $NbCr_2$/Cr Composites, Materials Transaction, JIM, 1997, 38(2), 155-162.
9. Reviere R., Sauthoff G., Jonson D. R., and Oliver B. F., Microstructure of Directionally Solidified Eutectic Based Fe (Al, Ta)/Fe_2Ta (Al) Alloys as a Function of Processing Condition, Intermetallics, 1997, 5(3), 161-172.
10. Liu C. T., Tortorelli P. F., Horton J. A., and Carmichael C. A., Effects of Alloy Additions on the Microstructure and Properties of Cr-Cr_2Nb Alloys, Materials Science and Engineering A, 1996, A214(1-2), 23-32.
11. Bewlay B. P. and Jackson M. R., Effect of Hf and Ti Additions on Microstructure and Properties of Cr_2Nb-Nb in situ Composites, Journal of Materials Research, 1996, 11(8), 1917-1922.

12. Takeyama M. and Liu C. T., Microstructure and Mechanical Properties of Laves-Phase Alloys Based on Cr_2Nb, Materials Science and Engineering A, 1991, A132(1-2), 61-66.
13. Kumar K. S., Pang L., Liu C. T., Horton J., and Kenik E. A., Structural Stability of the Laves-Phase Cr_2Ta in a Two-phase Cr-Cr_2Ta Alloy, Acta Materialia, 2000, 48(4), 911-923.
14. Takasugi T., Kumar K. S., Liu C. T., and Lee E. H., Microstructure and Properties of Two-phase Cr-Cr_2Nb, Cr-Cr_2Zr and Cr-Cr_2(Nb, Zr) Alloys, Materials Science and Engineering A, 1999, A260(1-2), 108-123.
15. Brady M. P., Zhu J. H., Liu C. T., Tortorelli P. F., Walker L. R., Mckamey C. G., and Wright J. L., Intermetallic Reinforced Cr Alloy for High-Temperature Use, Materials at High Temperatures, 1999, 16(4), 189-193.
16. Massalski T. B., Murray J. L., Bennett L. H., and Baker H. (Eds.), Binary Alloy Phase Diagram, American Society for Metals, Metals Park, OH, 1986.
17. Matsumoto Y., Fukumori J., Morinaga M., Furui M., Nambu T., and Sakaki T., Alloying Effect of 3D Transition Elements on the Ductility of Chromium, Scripta Materilia, 1996, 34(11), 1685-1689.
18. Provenzano V., Valiev R., Rickerby D. G., and Valdre G., Mechanical Properties of Nanostructured Chromium, Nanostructured Materials, 1999, 12(5), 1103-1108.
19. Morinaga M. and Nambu T., Effect of Surface Imperfections on the Ductility of Pure Chromium, Journal of Materials Science, 1995, 30(4), 1105-1110.
20. Liaw P. K., He Y. H., Brooks C. R., Liu C. T., L. Heatherly, and E. P. George, Investigation of The Microstructure and Mechanical Properties of Cr-Ta Composites Reinforced by Cr_2Ta Laves Phase, Proceedings of 12th Fossil Energy Conference, 2000, Knoxville, Tennessee, USA.

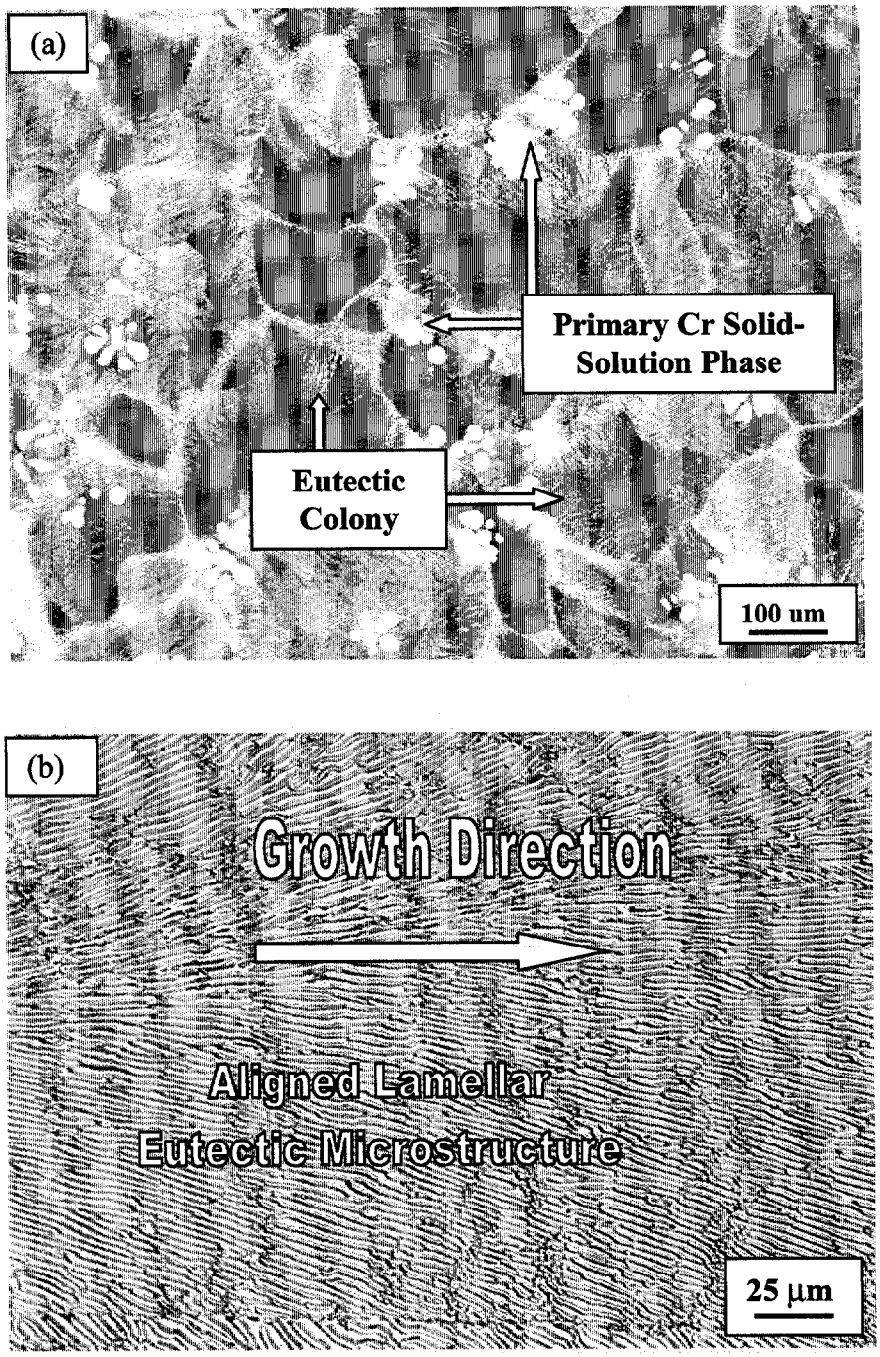

Figure 1 Microstructures of the drop-cast (a) and directionally-solidified (b) Cr-9.25 at.% Ta alloy along the longitudinal direction of the ingots

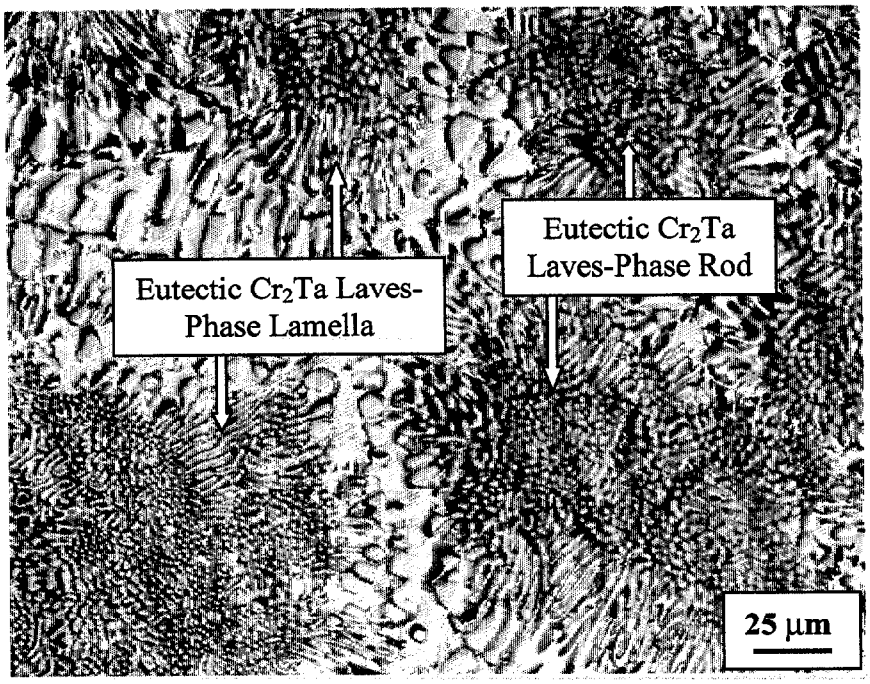

Figure 2 Cross-sectional microstructure of the directionally-solidified Cr-9.25 at.% Ta alloy

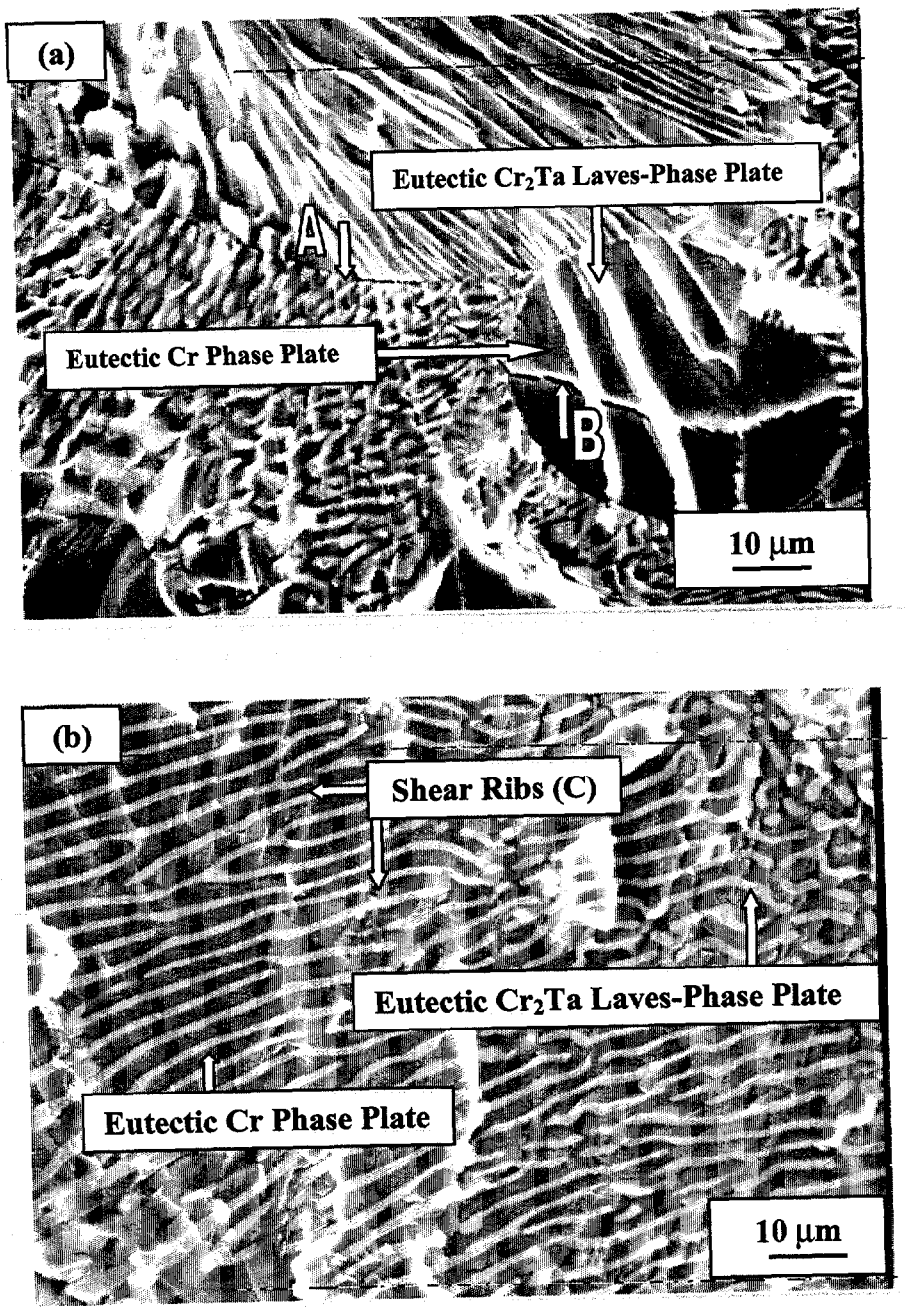

Figure 3 Fracture surfaces of the drop-cast (a) and directionally-solidified (b) Cr-9.25 at.% Ta alloy tensile-tested at room temperature

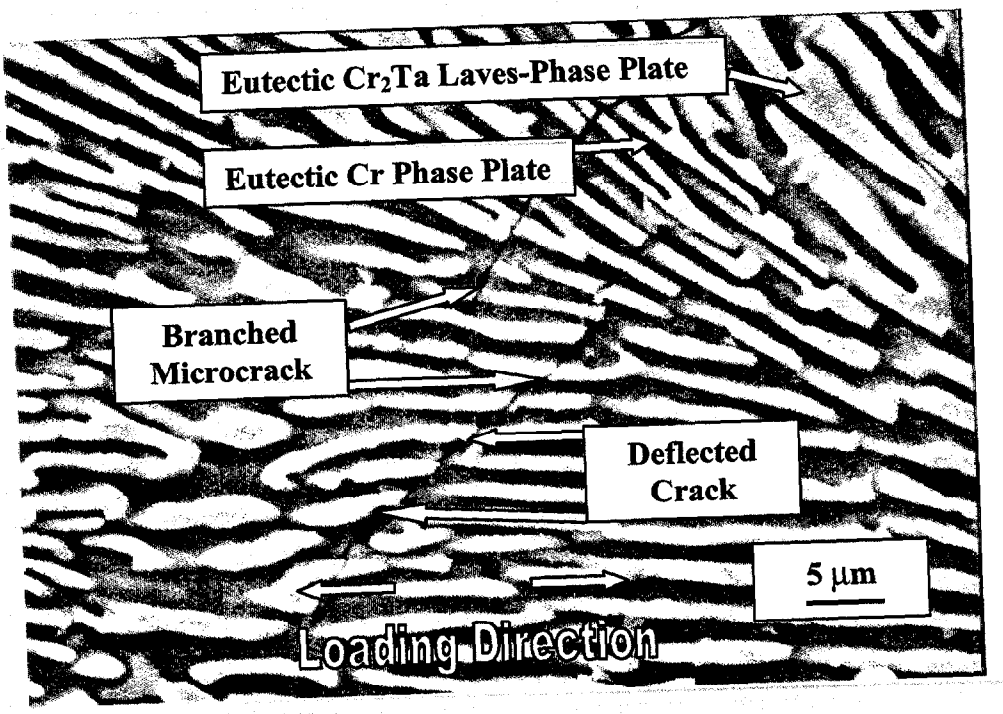

Figure 4 SEM micrograph of the microstructure along the longitudinal section of the directionally-solidified Cr-9.25 at.% Ta alloy tensile-tested at room temperature

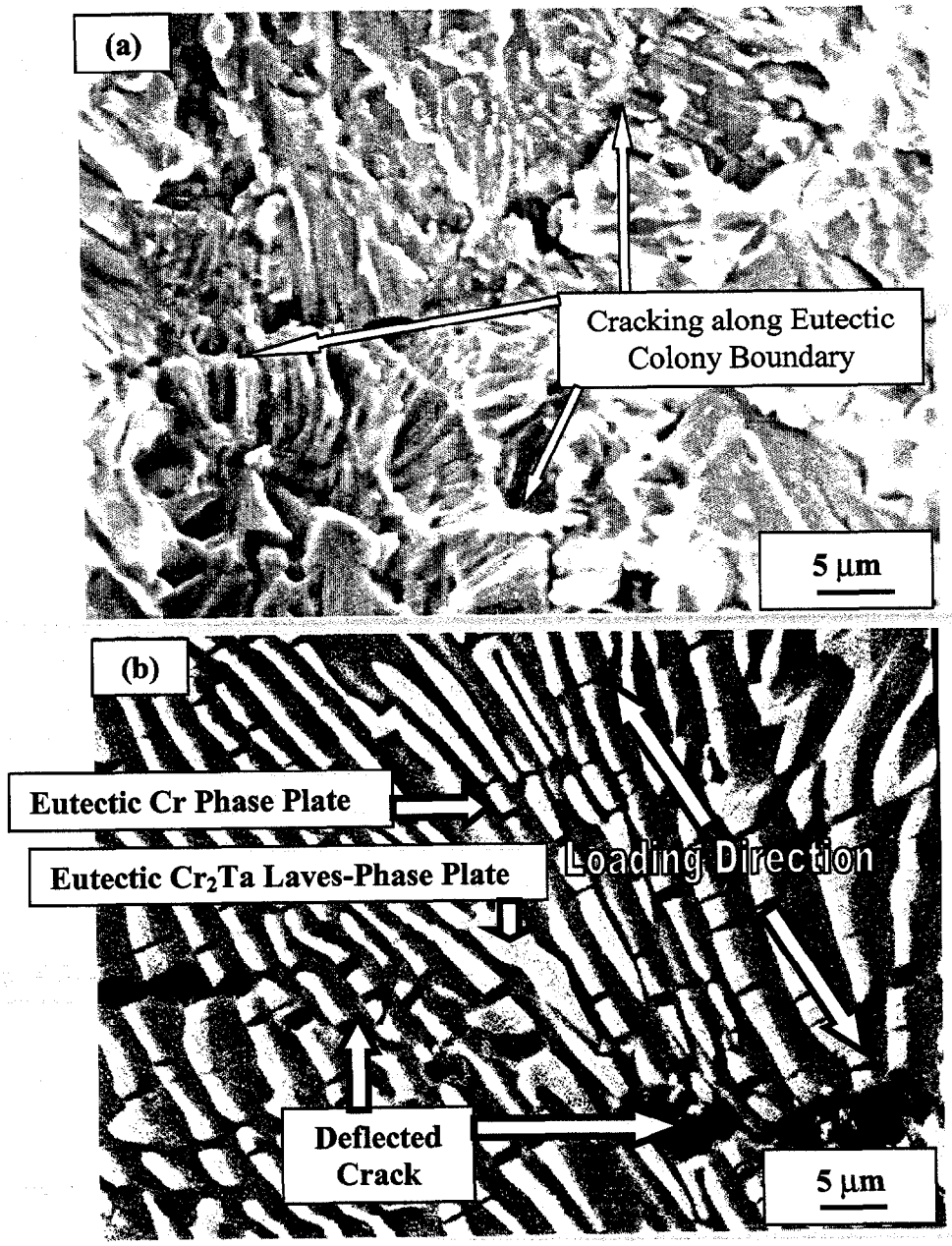

Figure 5 SEM micrographs of the microstructures along the longitudinal direction of the drop-cast (a) and directionally-solidified (b) Cr-9.25 at.% Ta alloy tensile-tested at 1,000°C

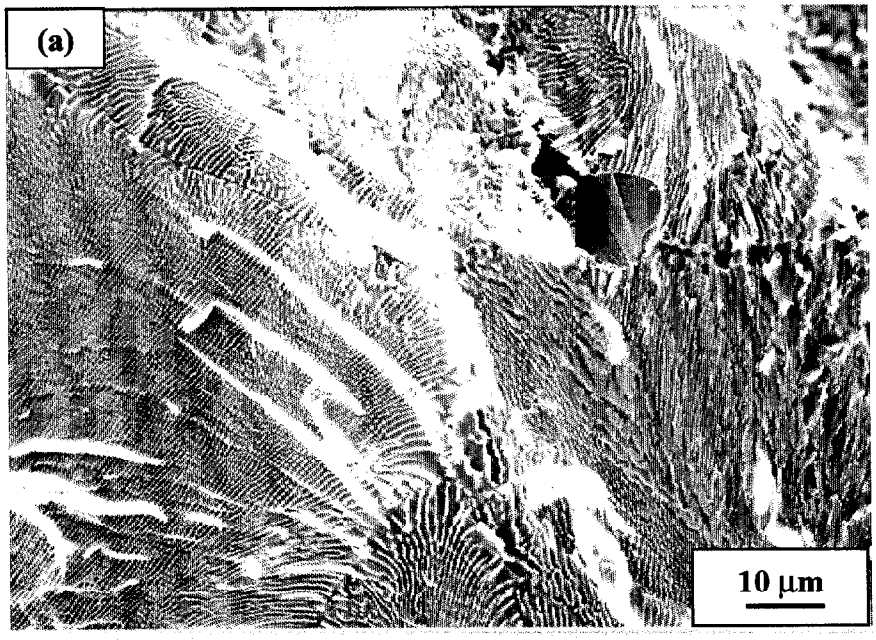
(a)
10 μm

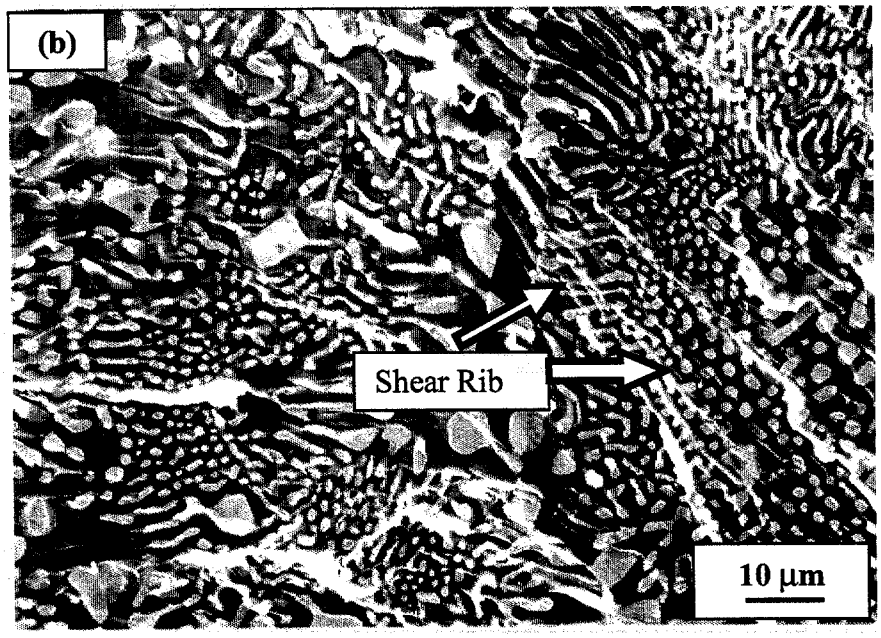
(b)
Shear Rib
10 μm

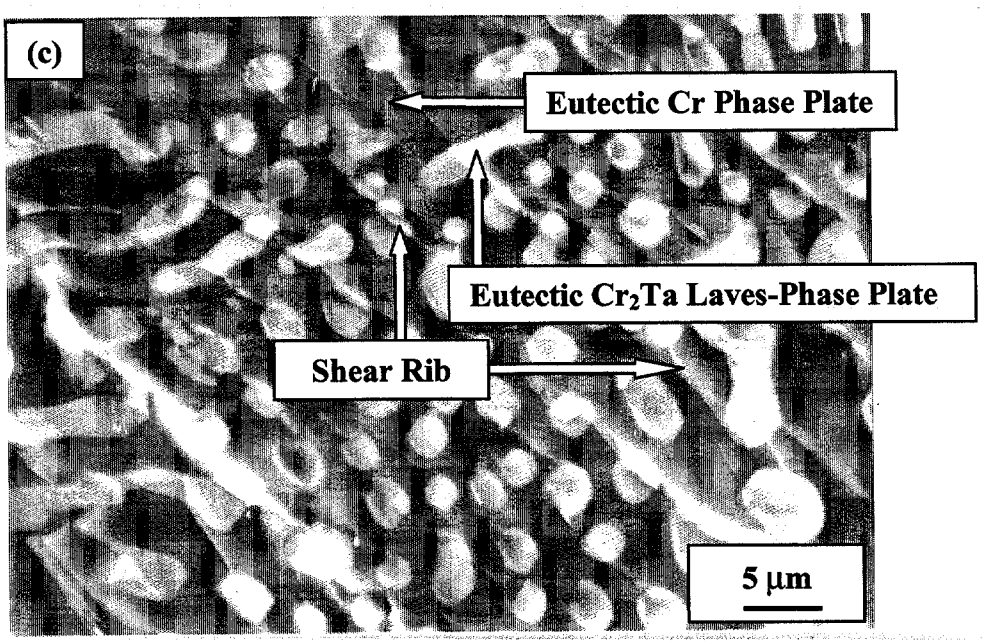

Figure 6 Fracture surfaces of the drop-cast (a) and directionally-solidified (b and c) Cr-9.25 at.% Ta alloy tested for fracture toughness

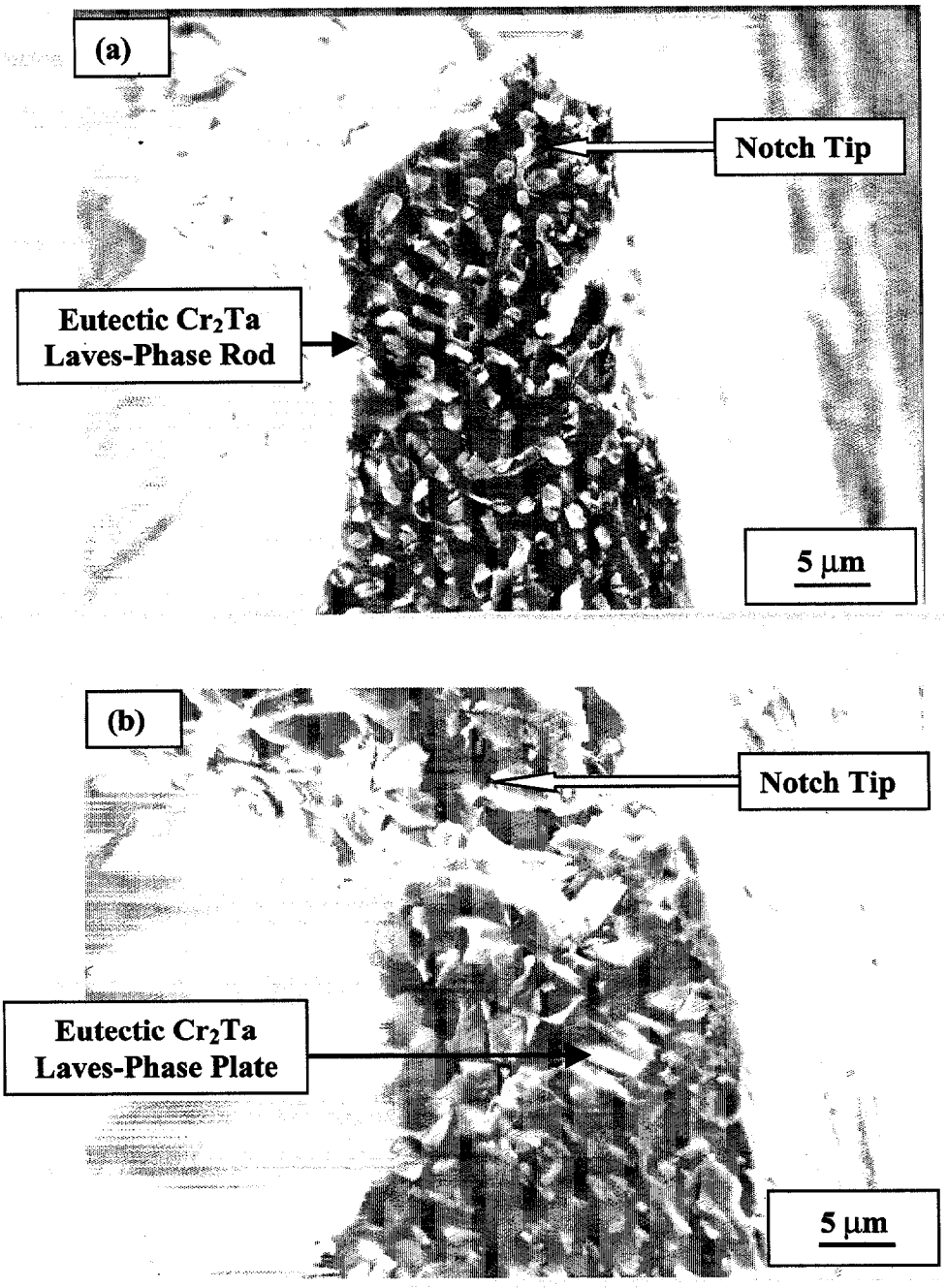

Figure 7 Fracture surfaces near the chevron-notch tips of the directionally-solidified Cr-9.25 at.% Ta alloy with fracture toughness values of 13.0 $MPa \cdot m^{1/2}$ (a) and > 15.0 $MPa \cdot m^{1/2}$ (b)

DISTRIBUTION

ALLISON GAS TURBINE DIVISION
P.O. Box 420
Indianapolis, IN 46206-0420
P. Khandelwal (Speed Code W-5)
R. A. Wenglarz (Speed Code W-16)

BABCOCK & WILCOX
Domestic Fossil Operations
20 South Van Buren Avenue
Barberton, OH 44023
M. Gold

BRITISH COAL CORPORATION
Coal Technology Development Division
Stoke Orchard, Cheltenham
Glocestershire, England GL52 4ZG
J. Oakey

CANADA CENTER FOR MINERAL & ENERGY TECHNOLOGY
568 Booth Street
Ottawa, Ontario
Canada K1A OG1
R. Winston Revie
Mahi Sahoo

COLORADO SCHOOL OF MINES
Department of Metallurgical Engineering
Golden, CO 80401
G. R. Edwards

DOE
DOE OAK RIDGE OPERATIONS
P. O. Box 2008
Building 4500N, MS 6269
Oak Ridge, TN 37831
M. H. Rawlins

DOE
National Energy Technology Laboratory
3610 Collins Ferry Road
P.O. Box 880
Morgantown, WV 26507-0880
D. C. Cicero
F. W. Crouse, Jr.
R. A. Dennis
N. T. Holcombe
W. J. Huber
T. J. McMahon
J. E. Notestein

DOE
National Energy Technology Laboratory
626 Cochrans Mill Road
P.O. Box 10940
Pittsburgh, PA 15236-0940
A. L. Baldwin
G. V. McGurl
U. Rao
L. A. Ruth
T. M. Torkos

DOE
OFFICE OF FOSSIL ENERGY
FE-72
19901 Germantown Road
Germantown, MD 20874-1290
F. M. Glaser

DOE
OFFICE OF BASIC ENERGY SCIENCES
Materials Sciences Division
ER-131 GTN
Washington, DC 20545
H. M. Kerch

FOSTER WHEELER DEVELOPMENT CORPORATION
Materials Technology Department
John Blizard Research Center
12 Peach Tree Hill Road
Livingston, NJ 07039
J. L. Blough

IDAHO NATIONAL ENGINEERING LABORATORY
P.O. Box 1625
Idaho Falls, ID 83415
R. N. Wright

LEHIGH UNIVERSITY
Materials Science & Engineering
Whitaker Laboratory
5 E. Packer Avenue
Bethlehem, PA 18015
J. N. DuPont

OAK RIDGE NATIONAL LABORATORY
P.O. Box 2008
Oak Ridge, TN 37831
M. P. Brady
P. T. Carlson
J. M. Crigger **(2 copies)**
R. R. Judkins
C. T. Liu
M. L. Santella
J. H. Schneibel
R. W. Swindeman
P. F. Tortorelli
I. G. Wright

PACIFIC NORTHWEST LABORATORY
P. O. Box 999, K3-59
Battelle Boulevard
Richland, WA 99352
R. N. Johnson

THE UNIVERSITY OF LIVERPOOL
Liverpool, United Kingdom
L69 3BX
A. R. Jones

THE WELDING INSTITUTE
Abington Hall, Abington
Cambridge CB1 6AL
United Kingdom
P. L. Threadgill

UNIVERSITY OF CALIFORNIA AT SAN DIEGO
Department of Applied Mechanics and Engineering Sciences
La Jolla, CA 92093-0411
B. K. Kad

UNIVERSITY OF TENNESSEE AT KNOXVILLE
Materials Science and Engineering Department
Knoxville, TN 37996
P. K. Liaw

WEST VIRGINIA UNIVERSITY
Department of Physics
Morgantown, WV 26506-6315\
B. R. Cooper